IMA Journal of Applied Mathematics (2005) **70**, 25–38
doi:10.1093/imamat/hxh061, Advanced Access Published on 17 December, 2004

Dedicated to Ray W. Ogden on the occasion of his 60th birthday

Dynamic extension of a compressible nonlinearly elastic membrane tube

H. A. ERBAY†
Department of Mathematics, Faculty of Science and Letters, Istanbul Technical University, Maslak 34469, Istanbul, Turkey

AND

V. H. TÜZEL‡
Department of Mathematics, Faculty of Science and Letters, Işık University, Maslak 34398, Istanbul, Turkey

The dynamic response of an isotropic compressible hyperelastic membrane tube is considered when one end is fixed and the other is subjected to a suddenly applied dynamic extension. The equations governing dynamic axially symmetric deformations of the membrane tube are presented for a general form of compressible isotropic elastic strain-energy function. Numerical results, obtained using a Godunov-type finite volume method and valid up to the time at which reflections occur at the fixed end of the tube, are given for two specific forms of the strain-energy function that characterizes a class of compressible elastomers (the Blatz–Ko model). The question of how the numerical results are related to the exact solution obtained for a limiting case is discussed.

Keywords: Blatz–Ko material; compressible; membrane tubes; nonlinear elasticity.

1. Introduction

The purpose of the present study is to investigate axially symmetric finite-amplitude wave propagation in a circular cylindrical compressible hyperelastic membrane tube when the tube is subjected to dynamic extension. We assume that one end of the tube is fixed and that the other end is subjected to a suddenly applied dynamic extension. We also assume that the resulting waves do not arrive at the fixed end of the tube over the time interval considered. The equations of motion along with compatibility conditions are written as a quasilinear hyperbolic system of first-order partial differential equations for a general form of elastic strain-energy function. Numerical results, obtained using a second-order Godunov method, are presented for two special models of Blatz–Ko compressible materials. A possible existence of shock waves is also discussed numerically.

In the case of incompressible hyperelastic materials the same problem has been studied by Tait & Zhong (1994a,b) and Tüzel & Erbay (2004). Tait & Zhong (1994a) have employed a numerical technique based on the method of characteristics and presented the numerical results for the Mooney–Rivlin incompressible material. In another study, Tait & Zhong (1994b) considered the same tube and, in addition to the extension, imposed a dynamical twist at the moving end. They have presented the

†Corresponding author. Email: erbay@itu.edu.tr
‡Present address: University of Minnesota, School of Mathematics, 127 Vincent Hall, 206 Church Street SE, Minneapolis, MN 55455, USA

numerical results for the neo-Hookean incompressible material. The discussion presented by Tüzel & Erbay (2004) has been set in a framework which differs in several aspects from that studied by Tait & Zhong (1994a). First, a nonlinear membrane theory has been derived by Tüzel & Erbay (2004) through an asymptotic expansion technique by starting from the three-dimensional equations of nonlinear elasticity theory, whereas an alternative approach based on the assumption that there exists a purely two-dimensional strain-energy function has been employed by Tait & Zhong (1994a) and the membrane has been considered as an elastic surface in three-dimensional space. Another difference between the studies by Tait & Zhong (1994a) and Tüzel & Erbay (2004) is the use of a second-order Godunov numerical method by Tüzel & Erbay (2004). Furthermore, a possible existence of shock waves is discussed by Tüzel & Erbay (2004). We refer the reader to Tüzel & Erbay (2004) for a comparison of the results obtained by Tüzel & Erbay (2004) with the results of Tait & Zhong (1994a).

It will be seen in the sequel that the analysis contained in the present study parallels quite closely that described by Tüzel & Erbay (2004). Regarding the problem of dynamic extension, the fundamental difference between Tüzel & Erbay (2004) and the present study arises in consideration of the tube material. Here we consider a circular cylindrical tube composed of a compressible hyperelastic material, whereas a membrane tube made of an incompressible hyperelastic material has been considered by Tüzel & Erbay (2004).

The purpose of Section 2 is to formulate the problem of dynamic extension for the membrane tube and is to present the equations corresponding to a limiting case of the loading problem. In the limiting case we assume that axial displacements are much larger than radial displacements and that a pure longitudinal wave can propagate without a coupled transverse wave. In Section 3, we present the numerical results obtained using a second-order Godunov method for two special Blatz–Ko materials. Also we discuss how the numerical results are related to the exact solutions of the limiting case.

2. Formulation of the problem and a limiting case

2.1 *Formulation of the problem*

We consider a circular cylindrical membrane of homogeneous isotropic compressible nonlinearly elastic material. Let (R, Θ, Z) and (r, θ, z) represent cylindrical polar coordinates associated with the undeformed and deformed configurations, respectively. In its (undeformed, stress free) natural configuration the membrane tube is defined by

$$R_i \leqslant R \leqslant R_i + H, \quad 0 \leqslant \Theta \leqslant 2\pi, \quad 0 \leqslant Z \leqslant L, \tag{2.1}$$

where R_i is the undeformed radius of the inner surface, H is the (uniform) thickness of the tube and L is the initial length of the tube. We suppose that the ends of the tube in the natural configuration are attached to rigid rings or discs of radius R_i. We also suppose that the end of the tube at $Z = L$ is kept fixed and the end originally at $Z = 0$ is displaced in the negative direction.

We record here the membrane equations in the dimensionless form without discussing their derivations since the extension from the incompressible case presented by Tüzel & Erbay (2004) to the compressible case is quite straightforward except for the constitutive relations. Henceforth non-dimensional variables are employed but, for convenience, the same letters are used to denote non-dimensional variables. Quantities with dimensions of length, stress and time are nondimensionalized by dividing by R_i, μ and $R_i(\rho_0/\mu)^{1/2}$, respectively, where ρ_0 is the mass density of the material of the body in the natural configuration and μ is the shear modulus for infinitesimal deformation from the undeformed state. The principal invariants I_k $(k = 1, 2, 3)$ of the right Cauchy–Green deformation

tensor are given by

$$I_1 = \Lambda_1^2 + \Lambda_2^2 + \Lambda_3^2, \quad I_2 = \Lambda_1^2\Lambda_2^2 + \Lambda_2^2\Lambda_3^2 + \Lambda_1^2\Lambda_3^2, \quad I_3 = \Lambda_1^2\Lambda_2^2\Lambda_3^2, \tag{2.2}$$

where Λ_1^2, Λ_2^2 and Λ_3^2 are the eigenvalues of the right Cauchy–Green deformation tensor (see Ogden, 1984). The scalar functions $\Lambda_k(R, Z, t)$ $(k = 1, 2, 3)$ are also called the principal stretches (Ogden, 1984). Note that $I_1 = I_2 = 3$ and $I_3 = 1$ in the reference configuration. The strain-energy density per unit undeformed volume for a compressible, isotropic and homogeneous hyperelastic material is given by $W = W(I_1, I_2, I_3)$ (Ogden, 1984), which can be also regarded as a function of the principal stretches: $W = W(\Lambda_1, \Lambda_2, \Lambda_3)$ where we use the same letter to indicate the revised functional dependence.

The dimensionless axial and radial coordinates of the deformed inner surface will be denoted by $f(Z, t)$ and $g(Z, t)$, respectively. The principal stretches of the inner surface in the deformed configuration are given by

$$\lambda_1 = \left[\left(f'\right)^2 + \left(g'\right)^2\right]^{\frac{1}{2}}, \quad \lambda_2 = g, \quad \lambda_3 = \frac{h}{H}, \tag{2.3}$$

where h represents the thickness of the deformed tube. Here and henceforth a prime denotes differentiation with respect to the dimensionless axial coordinate Z. Since the deformation is axially symmetric, the principal stretches λ_1, λ_2 and λ_3 are associated respectively with the axial, azimuthal and radial directions. If the values of the principal invariants for the deformed inner surface are denoted by i_k $(k = 1, 2, 3)$, the relationship between λ_k and i_k $(k = 1, 2, 3)$ is obtained by substituting λ_k and i_k for Λ_k and I_k, respectively, in (2.2). If the angle between the radial direction and the tangent of the deformed inner surface is denoted by $\beta(Z, t)$, we have

$$f' = \lambda_1 \sin\beta, \quad g' = \lambda_1 \cos\beta. \tag{2.4}$$

The constitutive relations are expressed in terms of the principal components of Biot stress and principal stretches. A detailed discussion of the Biot stress tensor is given by Ogden (1984). For the present problem the principal Biot stresses $T_k(Z, t)$ $(k = 1, 2, 3)$ for the deformed inner surface are conjugate to the principal stretches λ_k $(k = 1, 2, 3)$ and

$$T_1 = \left.\frac{\partial W}{\partial \Lambda_1}\right|_{\Lambda_k=\lambda_k}, \quad T_2 = \left.\frac{\partial W}{\partial \Lambda_2}\right|_{\Lambda_k=\lambda_k}, \quad T_3 = \left.\frac{\partial W}{\partial \Lambda_3}\right|_{\Lambda_k=\lambda_k} \equiv 0, \tag{2.5}$$

which are associated with the axial, azimuthal and radial directions, respectively. It follows from (2.5) and (2.2) that

$$W_1 + \left(\lambda_1^2 + \lambda_2^2\right) W_2 + \lambda_1^2\lambda_2^2 W_3 = 0, \tag{2.6}$$

where, for the sake of brevity, the notation $W_l = \partial W/\partial I_l|_{I_k=i_k}$ $(l, k = 1, 2, 3)$ is used.

In the absence of the normal and tangential surface tractions on both the inner and outer surfaces, the equations of motion are given in the form

$$\frac{\partial}{\partial Z}\left(T_1 \cos\beta\right) - T_2 = \frac{\partial^2 g}{\partial t^2}, \tag{2.7}$$

$$\frac{\partial}{\partial Z}\left(T_1 \sin\beta\right) = \frac{\partial^2 f}{\partial t^2}, \tag{2.8}$$

as in (4.1)–(4.2) of Tüzel & Erbay (2004). If we set

$$u = \frac{\partial g}{\partial t}, \qquad v = \frac{\partial f}{\partial t}, \tag{2.9}$$

we can write the following compatibility equations:

$$\frac{\partial(\lambda_1 \cos\beta)}{\partial t} = \frac{\partial u}{\partial Z}, \qquad \frac{\partial(\lambda_1 \sin\beta)}{\partial t} = \frac{\partial v}{\partial Z}, \qquad \frac{\partial \lambda_2}{\partial t} = u. \tag{2.10}$$

If these compatibility equations are combined with the equations of motion given by (2.7) and (2.8), the governing equations may be rewritten in the vector form

$$\frac{\partial \mathbf{Q}}{\partial t} + \frac{\partial \mathbf{H}(\mathbf{Q})}{\partial Z} + \mathbf{B}(\mathbf{Q}) = \mathbf{0}, \tag{2.11}$$

where

$$\begin{aligned} &\mathbf{Q} = \{\lambda_1 \cos\beta, \lambda_1 \sin\beta, \lambda_2, u, v\}^{\mathrm{T}}, \quad \mathbf{H} = -\{u, v, 0, T_1 \cos\beta, T_1 \sin\beta\}^{\mathrm{T}}, \\ &\mathbf{B} = -\{0, 0, u, -T_2, 0\}^{\mathrm{T}}. \end{aligned} \tag{2.12}$$

The above system can be written in the form

$$\frac{\partial \mathbf{Q}}{\partial t} + \mathbf{A}(\mathbf{Q}) \frac{\partial \mathbf{Q}}{\partial Z} + \mathbf{B} = \mathbf{0}, \tag{2.13}$$

where $\mathbf{A}(\mathbf{Q}) \equiv \partial \mathbf{H}(\mathbf{Q})/\partial \mathbf{Q}$ is the 5×5 Jacobian matrix with the non-zero entries given by

$$\begin{aligned} &A_{14} = -1, \qquad A_{25} = -1, \qquad A_{41} = -\frac{\partial T_1}{\partial \lambda_1} \cos^2\beta - \frac{T_1}{\lambda_1} \sin^2\beta, \\ &A_{42} = A_{51} = -\left(\frac{T_1}{\lambda_1} - \frac{\partial T_1}{\partial \lambda_1}\right) \sin\beta \cos\beta, \qquad A_{43} = -\frac{\partial T_1}{\partial \lambda_2} \cos\beta, \\ &A_{52} = -\frac{\partial T_1}{\partial \lambda_1} \sin^2\beta - \frac{T_1}{\lambda_1} \cos^2\beta, \qquad A_{53} = -\frac{\partial T_1}{\partial \lambda_2} \sin\beta. \end{aligned} \tag{2.14}$$

The eigenvalues of $\mathbf{A}$ are $\Delta_0 = 0, \quad \Delta_{\pm 1} = \pm C_L, \quad \Delta_{\pm 2} = \pm C_T$, where C_L and C_T are given by

$$C_L^2 = \frac{\partial T_1}{\partial \lambda_1}, \qquad C_T^2 = \frac{T_1}{\lambda_1}. \tag{2.15}$$

System (2.13) is strictly hyperbolic when the wave speeds are real and distinct (i.e. $C_L^2 > 0$, $C_T^2 > 0$ and $C_L \neq C_T$). Later it will be shown from numerical results that C_L and C_T represent the speeds of an essentially longitudinal wave and an essentially transverse wave, respectively.

To proceed with our analysis further, the boundary and initial conditions for the problem can be given as follows. Since the initial configuration is the reference configuration

$$g(Z, 0) = 1, \qquad f(Z, 0) = Z, \tag{2.16}$$

one can write the initial conditions in the form

$$\lambda_1(Z, 0) = \lambda_2(Z, 0) = 1, \qquad \beta(Z, 0) = \pi/2, \qquad u(Z, 0) = v(Z, 0) = 0, \tag{2.17}$$

for $0 \leqslant Z \leqslant L$. The boundary conditions for the present problem are

$$\begin{array}{lll} \lambda_2(0,t) = 1, & u(0,t) = 0, & v(0,t) = -v_0, \\ \lambda_1(L,t) = 1, & \beta(L,t) = \pi/2 & \end{array} \tag{2.18}$$

for $t > 0$, where v_0 denotes the constant velocity imposed at $Z = 0$. Here we assume that the waves do not arrive in the end $Z = L$ over the time interval considered.

Up to this point the strain at energy function W has remained arbitrary. It is not clear whether the wave speeds are real and distinct. In order to obtain precise results we consider two kinds of compressible material models studied in experiments by Blatz & Ko (1962), both of which have received much attention in the literature: the Blatz–Ko *foamed*, polyurethane elastomer and the Blatz–Ko *solid*, polyurethane elastomer. A detailed discussion of the Blatz–Ko material models is given by Beatty (1987).

2.1.1 *Blatz–Ko foamed, polyurethane elastomer.* The non-dimensional form of the strain-energy function corresponding to the Blatz–Ko foamed, polyurethane elastomer is

$$W(I_1, I_2, I_3) = \tfrac{1}{2}(I_2 I_3^{-1} + 2I_3^{1/2} - 5) \tag{2.19}$$

or, equivalently,

$$W(\Lambda_1, \Lambda_2, \Lambda_3) = \tfrac{1}{2}(\Lambda_1^{-2} + \Lambda_2^{-2} + \Lambda_3^{-2} + 2\Lambda_1\Lambda_2\Lambda_3 - 5). \tag{2.20}$$

Then, the principal Biot stresses T_1 and T_2 given by (2.5) are computed as

$$T_1 = -\lambda_1^{-3} + \lambda_2\lambda_3, \quad T_2 = -\lambda_2^{-3} + \lambda_1\lambda_3. \tag{2.21}$$

We now use the restriction given by (2.6) to eliminate λ_3 from these equations. For the Blatz–Ko model (2.19), equation (2.6) gives λ_3 in the form

$$\lambda_3 = (\lambda_1\lambda_2)^{-1/3}. \tag{2.22}$$

Then we can express T_1 and T_2 as

$$T_1 = -\lambda_1^{-3} + \lambda_1^{-1/3}\lambda_2^{2/3}, \quad T_2 = -\lambda_2^{-3} + \lambda_1^{2/3}\lambda_2^{-1/3}. \tag{2.23}$$

It follows from (2.15) that

$$C_L^2 = -\tfrac{1}{3}\lambda_1^{-4/3}\lambda_2^{2/3} + 3\lambda_1^{-4}, \quad C_T^2 = \lambda_1^{-4/3}\lambda_2^{2/3} - \lambda_1^{-4}. \tag{2.24}$$

If we introduce a new function $\alpha(\lambda_1, \lambda_2)$ through the relation

$$\alpha(\lambda_1, \lambda_2) = \lambda_1^{-4} - \tfrac{1}{3}\lambda_1^{-4/3}\lambda_2^{2/3}, \tag{2.25}$$

we can easily deduce that

$$C_L^2 = 2\lambda_1^{-4} + \alpha, \quad C_T^2 = 2\lambda_1^{-4} - 3\alpha, \quad C_L^2 - C_T^2 = 4\alpha. \tag{2.26}$$

Then we observe that $C_L^2 > C_T^2 > 0$ whenever

$$0 < \alpha(\lambda_1, \lambda_2) < \frac{2}{3}\lambda_1^{-4}. \tag{2.27}$$

2.1.2 *Blatz–Ko solid, polyurethane elastomer.* The non-dimensional form of the strain-energy function corresponding to the Blatz–Ko solid, polyurethane elastomer is

$$W(I_1, I_2, I_3) = \frac{1}{2}\left[I_1 - 3 - \frac{2}{q}(I_3^{q/2} - 1)\right], \tag{2.28}$$

or, equivalently,

$$W(\Lambda_1, \Lambda_2, \Lambda_3) = \frac{1}{2}\left\{(\Lambda_1^2 + \Lambda_2^2 + \Lambda_3^2 - 3) - \frac{2}{q}[(\Lambda_1\Lambda_2\Lambda_3)^q - 1]\right\}, \tag{2.29}$$

where $q < 0$. For simplicity, we shall restrict our analysis to a Blatz–Ko membrane tube for which $q = -2$. Then, the principal Biot stresses T_1 and T_2 given by (2.5) are calculated as

$$T_1 = \lambda_1 - \lambda_1^{-3}\lambda_2^{-2}\lambda_3^{-2}, \quad T_2 = \lambda_2 - \lambda_1^{-2}\lambda_2^{-3}\lambda_3^{-2}. \tag{2.30}$$

We now use the restriction given by (2.6) to eliminate λ_3 from these equations. For the Blatz–Ko model (2.28) with $q = -2$, (2.6) gives λ_3^2 in the form

$$\lambda_3^2 = \lambda_1^{-1}\lambda_2^{-1}. \tag{2.31}$$

Then we can rewrite

$$T_1 = \lambda_1 - \lambda_1^{-2}\lambda_2^{-1}, \quad T_2 = \lambda_2 - \lambda_1^{-1}\lambda_2^{-2}. \tag{2.32}$$

It follows from (2.15) that

$$C_L^2 = 1 + 2\lambda_1^{-3}\lambda_2^{-1}, \quad C_T^2 = 1 - \lambda_1^{-3}\lambda_2^{-1}, \quad C_L^2 - C_T^2 = 3\lambda_1^{-3}\lambda_2^{-1}, \tag{2.33}$$

which imply $C_L^2 > C_T^2 > 0$ provided $\lambda_1^3\lambda_2 > 1$.

2.2 *A limiting case*

A limiting case has been considered by Tait & Zhong (1994a,b) in which the governing equations essentially reduce to those for a stretched string. The closed form solutions obtained for the approximate set of equations have been used as a check on the numerical results presented for the full set of equations. We now follow a similar approach and use the exact solutions obtained for the limiting case as a check on the numerical results. Specifically, we deal with the limiting case of the loading problem when axial displacements are much larger than radial displacements. In other words, for the moment, we assume that a pure longitudinal wave can propagate without a coupled transverse wave. Then in the motion we approximate $g, \lambda_2, u, g', \lambda_1$ and β by $g = 1, \lambda_2 = 1, u = 0, g' = 0, \lambda_1 = f'$ and $\beta = \pi/2$, respectively. Then the system (2.11) reduces to

$$\frac{\partial}{\partial t}\begin{pmatrix}\lambda_1 \\ v\end{pmatrix} + \begin{pmatrix}0 & -1 \\ -c^2 & 0\end{pmatrix}\frac{\partial}{\partial Z}\begin{pmatrix}\lambda_1 \\ v\end{pmatrix} = \mathbf{0}, \tag{2.34}$$

where

$$c^2 = \frac{\mathrm{d}T_1(\lambda_1)}{\mathrm{d}\lambda_1}, \quad T_1 = \frac{\mathrm{d}W(\lambda_1)}{\mathrm{d}\lambda_1}, \tag{2.35}$$

and $\pm c(\lambda_1)$ are the wave speeds associated with pure stretching waves. The system (2.34) is the same as that given in (5.1) of Tait & Zhong (1994a) for the Mooney–Rivlin incompressible material. We consider the initial conditions

$$v(Z,0) = 0, \quad \lambda_1(Z,0) = 1, \tag{2.36}$$

for $0 \leqslant Z \leqslant L$ and the boundary conditions

$$v(0,t) = -v_0, \quad \lambda_1(L,t) = 1 \quad t > 0\,, \tag{2.37}$$

(Tait & Zhong, 1994a,b). The explicit solution of the problem defined by (2.34)–(2.37) has been given by Tait & Zhong (1994b) for the neo-Hookean incompressible material. A similar approach is also valid for the compressible case under the restriction $dc(\lambda_1)/d\lambda_1 < 0$, which is satisfied for both models of the Blatz–Ko material within the range of finite deformation considered in the numerical experiments of Section 3.

The solution consists of two constant regions joined by a simple expansion fan and takes the following form in our notation.

(i) If $0 \leqslant Z \leqslant c^*t$ where $c^* = c(\lambda_1^*)$ and λ_1^* is determined by the equation

$$v_0 = \int_1^{\lambda_1^*} c(\lambda_1)\,\mathrm{d}\lambda_1, \tag{2.38}$$

the solution is given by

$$\lambda_1 = \lambda_1^*, \quad v = v_0. \tag{2.39}$$

(ii) If $c^*t \leqslant Z \leqslant c_0 t$ where $c_0 = c(1)$, the solution is given by

$$c^2(\lambda_1) = \left(\frac{Z}{t}\right)^2, \quad v = -\int_1^{\lambda_1} c(\tau)\,\mathrm{d}\tau, \tag{2.40}$$

where first λ_1 is calculated from $(2.40)_1$ and then substituting the result into $(2.40)_2$ v is calculated.

(iii) If $c_0 t \leqslant Z \leqslant L$, the solution is given by

$$\lambda_1 = 1, \quad v = 0. \tag{2.41}$$

For further details on this solution see Tait & Zhong (1994b).

3. Numerical results

Since the high nonlinearity of the equations and the presence of the source terms rule out analytical solutions, the initial and boundary-value problem defined by (2.11), (2.12), (2.17) and (2.18) is solved numerically for the Blatz–Ko models (2.19) and (2.28) by using a modified second-order Godunov method. The basic idea of Godunov-type methods is to compose the global solution by the exact or approximate solutions of local Riemann problems. The second-order method replaces the piecewise constant representation of the solution in the first-order method by a piecewise linear representation. Algorithms of this type were first introduced by Van Leer (1979). For an application of the numerical method to nonlinear elasticity we refer to Haddow & Jiang (2001).

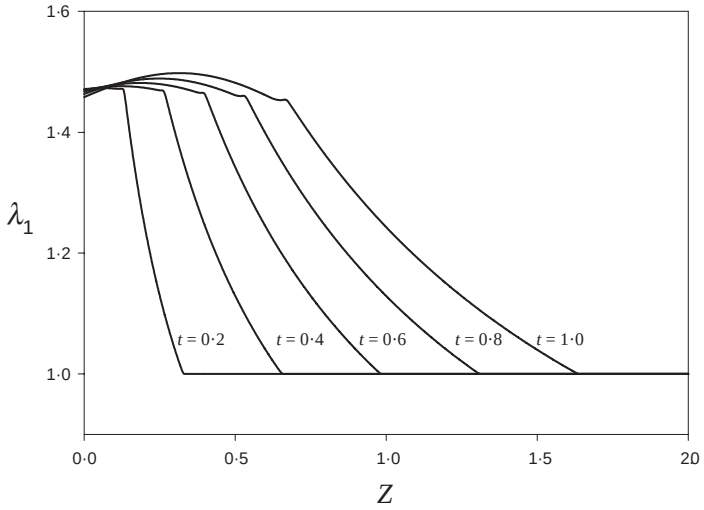

FIG. 1. λ_1 as a function of Z at various times for the Blatz–Ko model (2.19). $L = 2,\ v_0 = 0{\cdot}5$.

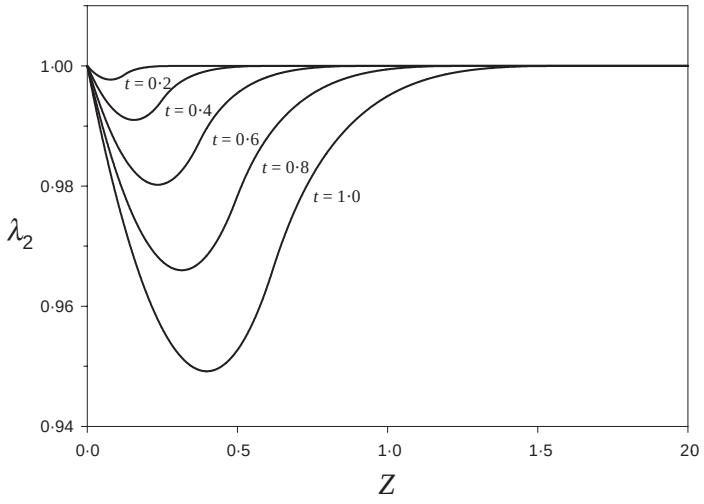

FIG. 2. λ_2 as a function of Z at various times for the Blatz–Ko model (2.19). $L = 2,\ v_0 = 0{\cdot}5$.

We first consider a membrane tube composed of the Blatz–Ko foamed, polyurethane elastomer. After some numerical experiments we observe that the condition (2.27) is satisfied if $v_0 \leqslant 0{\cdot}714$. We apply the numerical scheme for the parameter values $L = 2$, $v_0 = 0{\cdot}5$. Figures 1 and 2 show the values of λ_1 and λ_2 as functions of Z at various times for the Blatz–Ko model (2.19). A comparison of the numerical results with those given in Figs 1 and 2 of Tüzel & Erbay (2004) shows that the numerical results for compressible materials are qualitatively similar to those for incompressible materials. Recall that we take the undeformed configuration as the initial configuration. Therefore the membrane is undisturbed ahead of the fastest wave. The leading edge of the fastest wave travels at speed $C_L|_{\lambda_1=\lambda_2=1} = \sqrt{8/3}$.

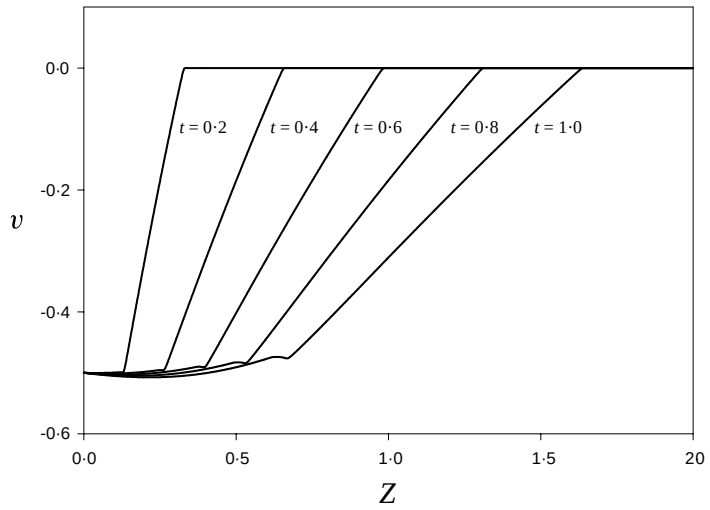

FIG. 3. v as a function of Z at various times for the Blatz–Ko model (2.19). $L = 2,\ v_0 = 0{\cdot}5$.

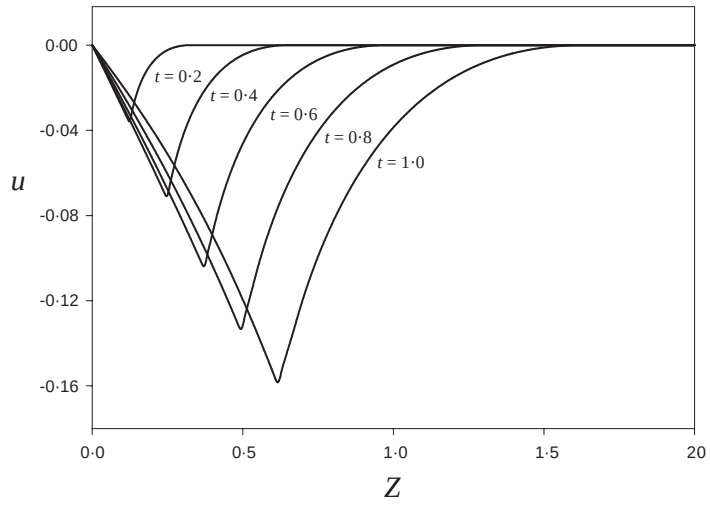

FIG. 4. u as a function of Z at various times for the Blatz–Ko model (2.19). $L = 2,\ v_0 = 0{\cdot}5$.

At impact λ_1 jumps from its initial value 1 to a new value about 1·5. As in the incompressible case (Tait & Zhong, 1994a; Tüzel & Erbay, 2004), the discontinuity in λ_1 does not propagate and the impact is followed by an expansion wave. An expansion wave of λ_1 joins the undisturbed region to the region where interaction between the waves takes place.

Figures 3 and 4 show the values of v and u as functions of Z at various times for the Blatz–Ko model (2.19). Note that the governing equations cannot be separated into two uncoupled systems which govern the propagation of a longitudinal wave (associated with f' and v) and a transverse wave (associated with g' and u), respectively. It follows from (2.3) and (2.24) that the wave speeds C_L and C_T are functions

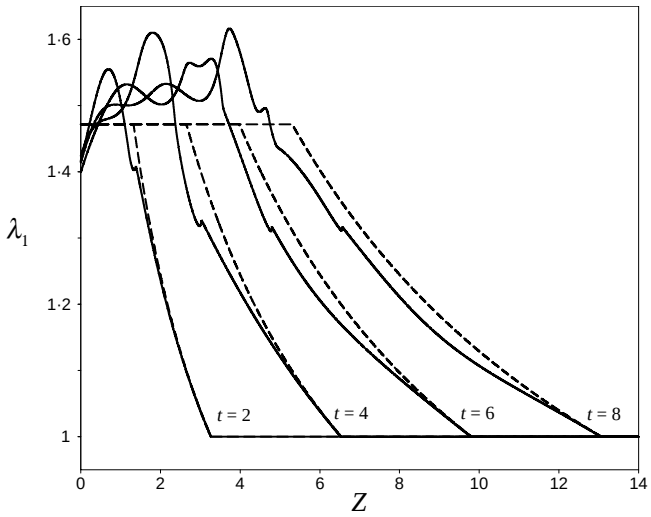

FIG. 5. λ_1 as a function of Z at various times for the Blatz–Ko model (2.19). The dashed lines represent the simplified solution obtained from the limiting case. $L = 14,\ v_0 = 0{\cdot}5$.

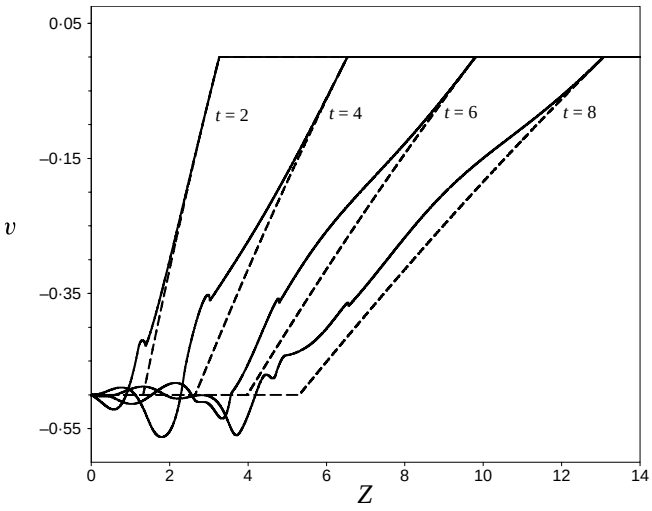

FIG. 6. v as a function of Z at various times for the Blatz–Ko model (2.19). The dashed lines represent the simplified solution obtained from the limiting case. $L = 14,\ v_0 = 0{\cdot}5$.

of f' and g' so that they are also coupled. Therefore a pure longitudinal or transverse wave cannot exist and interaction takes place. The results shown in Figs 3 and 4 indicate that both essentially longitudinal wave and essentially transverse wave are acceleration waves and exhibit no discontinuities of v and u. The discontinuity in v' propagates faster than the u' discontinuity. This result indicates that the wave with speed C_L is an essentially v wave whereas the wave with speed C_T is an essentially u wave. The v wave exhibits a perturbation as it passes through the u' discontinuity and an additional discontinuity in v'

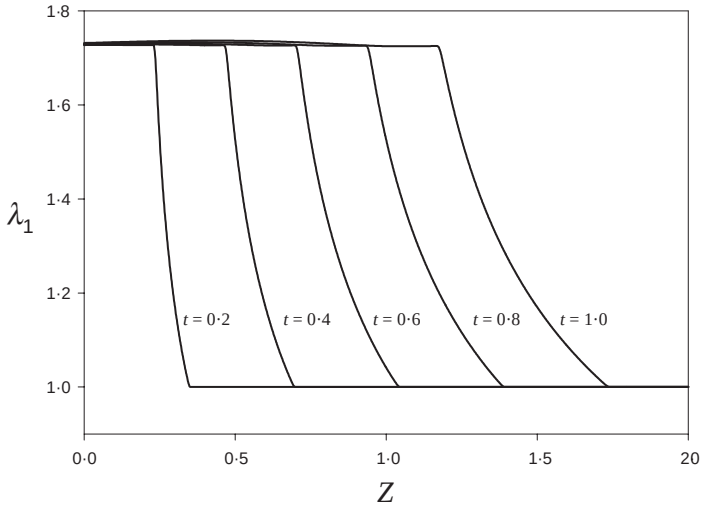

FIG. 7. λ_1 as a function of Z at various times for the Blatz–Ko model (2.28). $L = 2,\ v_0 = 1$.

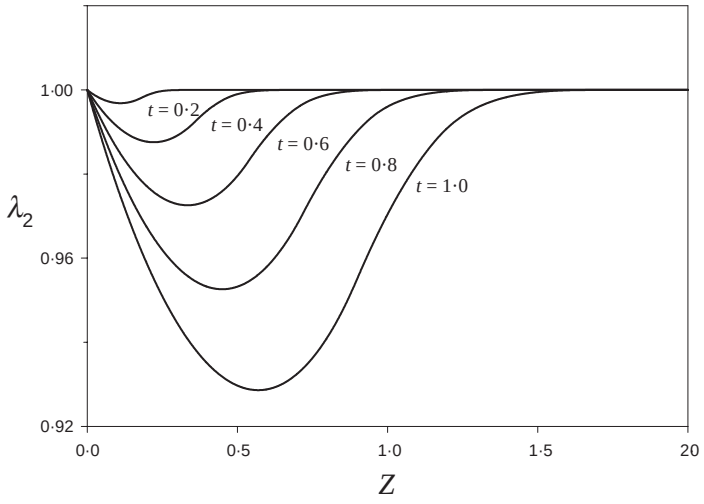

FIG. 8. λ_2 as a function of Z at various times for the Blatz–Ko model (2.28). $L = 2,\ v_0 = 1$.

results from the discontinuity in u'. This is a direct consequence of the coupling of the waves. However, this additional discontinuity in v' is not visible for the Blatz–Ko compressible material (2.19) as much as that in the case of the Mooney–Rivlin incompressible material (see Fig. 3 of Tüzel & Erbay, 2004).

We now ask whether the discontinuities in λ_1' and v' are transformed into the discontinuities in λ_1 and v, respectively, over large time and space intervals for the Blatz–Ko model (2.19). In order to investigate numerically whether shocks will eventually form we repeat the numerical experiment for greater values of time t. In these experiments we also increase the value of L to prevent from the reflected wave modifying the behaviour. In Figs 5 and 6 we show the values of λ_1 and v as functions of Z at various

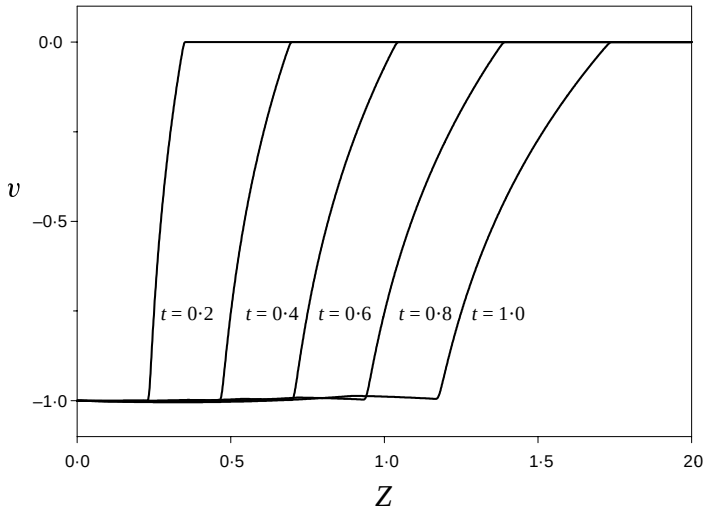

FIG. 9. v as a function of Z at various times for the Blatz–Ko model (2.28). $L = 2,\ v_0 = 1$.

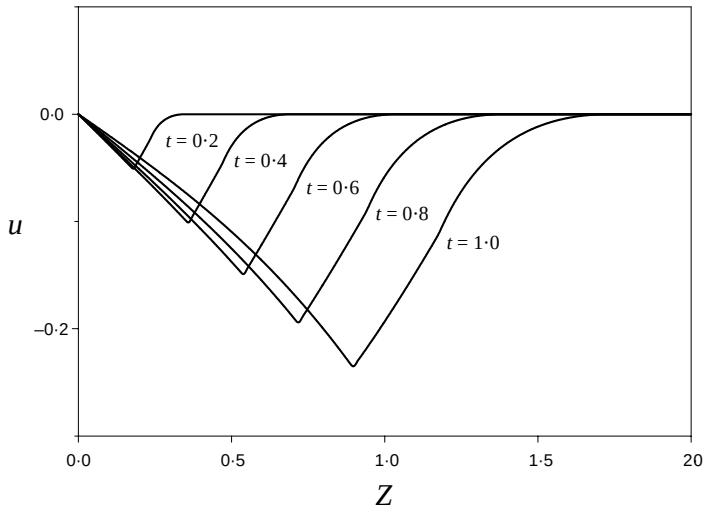

FIG. 10. u as a function of Z at various times for the Blatz–Ko model (2.28). $L = 2,\ v_0 = 1$.

times for $L = 14$. The solid line in each figure indicates the numerical results obtained by solving the exact equations as in the previous figures. However, the dashed lines in the figures indicate the exact solutions of the limiting case, (2.39)–(2.41). That is, in Figs 5 and 6 we compare the numerical solutions of the full set of equations with the analytical solutions given by (2.39)–(2.41). In the limiting case the longitudinal wave is an acceleration wave and exhibits no discontinuities of λ_1 or v. As Z increases the numerical solution of the full equations approaches the exact solution of the limiting case. These results indicate that qualitative differences between the results for the original problem and the limiting case result from the coupled transverse wave. Note that the numerical results in Figs 5 and 6 of Tüzel &

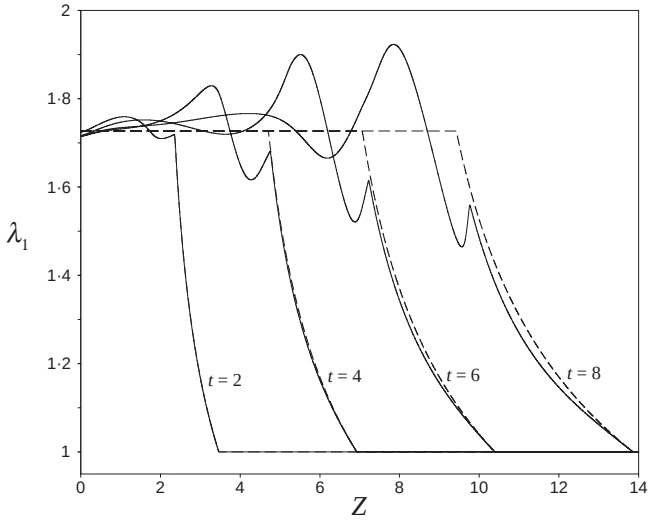

FIG. 11. λ_1 as a function of Z at various times for the Blatz–Ko model (2.28). The dashed lines represent the simplified solution obtained from the limiting case. $L = 14,\ v_0 = 1$.

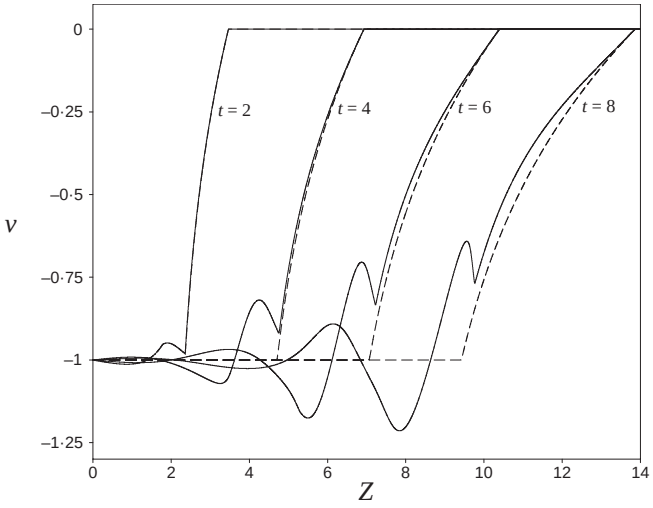

FIG. 12. v as a function of Z at various times for the Blatz–Ko model (2.28). The dashed lines represent the simplified solution obtained from the limiting case. $L = 14,\ v_0 = 1$.

Erbay (2004) indicate that a shock wave forms as time increases for the Mooney–Rivlin incompressible material. However, although a formal proof of the non-existence of shock waves is not presented here, the numerical results presented in Figs 5 and 6 strongly indicate that a shock wave does not form for the Blatz–Ko model (2.19). For a discussion of the transition from acceleration wave to shock wave in the case of a pure longitudinal wave we refer to Fu & Scott (1991).

We now consider a membrane tube composed of the Blatz–Ko solid, polyurethane elastomer. We

apply the numerical scheme for the parameter values $L = 2$, $v_0 = 1$ and $q = -2$. Figures 7–10 show the values of λ_1, λ_2, v, u as functions of Z at various values of t for the Blatz–Ko model (2.28). The leading edge of the fastest wave travels at speed $C_L|_{\lambda_1=\lambda_2=1} = \sqrt{3}$. Except for a few quantitative differences, it is seen that the overall physical response for the Blatz–Ko model (2.28) is not greatly different from the impact behaviour found for the Blatz–Ko model (2.19). In Figs 11 and 12 we compare the numerical solutions of the full set of equations with the analytical solutions obtained from the limiting case for the Blatz–Ko model (2.28). In these figures, the curves corresponding to the case $t = 2$ are indistinguishable. We observe that the remarks made above for the Blatz–Ko model (2.19) are not affected if the Blatz–Ko model (2.28) is considered and that both models give rise to the same qualitative behaviour. In particular, the qualitative differences between the numerical and analytical results presented in Figs 11 and 12 indicate the coupled simultaneous propagation of longitudinal and transverse waves.

REFERENCES

BEATTY, M. F. (1987) Topics in finite elasticity: hyperelasticity of rubber, elastomers, and biological tissues–with examples. *Appl. Mech. Rev.*, **40**, 1699–1734.

BLATZ, P. J. & KO, W. L. (1962) Applications of finite elasticity theory to deformation of rubbery materials. *Trans. Soc. Rheology*, **6**, 223–251.

FU, Y. B. & SCOTT, N. H. (1991) The transition from acceleration wave to shock wave. *Int. J. Engng Sci.*, **29**, 617–624.

HADDOW, J. B. & JIANG, L. (2001) Finite amplitude azimuthal shear waves in a compressible hyperelastic solid. *ASME J. Appl. Mech.*, **68**, 145–152.

OGDEN, R. W. (1984) *Non-linear Elastic Deformations*. Chichester: Ellis Horwood.

TAIT, R. J. & ZHONG, J. L. (1994a) Wave propagation in a non-linear elastic tube. *Bull. Tech. Univ.*, **47**, 127–150.

TAIT, R. J. & ZHONG, J. L. (1994b) Dynamic extension and twist of a non-linear elastic tube. *Int. J. Non-Linear Mech.*, **30**, 887–898.

TÜZEL, V. H. & ERBAY, H. A. (2004) The dynamic response of an incompressible non-linearly elastic membrane tube subjected to a dynamic extension. *Int. J. Non-Linear Mech.*, **39**, 515–537.

VAN LEER, B. (1979) Towards the ultimate conservative difference scheme. V. A second-order sequel to Godunov's method. *J. Comput. Phys.*, **32**, 101–136.